Effect of Anterior Commisure - Posterior Commisure Reorientation for 3D Aneurysm Segmentation in the Brain

Richard Ryan
Department of Informatics
Institut Teknologi Sepuluh Nopember
Surabaya, Indonesia
5025211141@student.its.ac.id

Riyanarto Sarno
Department of Informatics
Institut Teknologi Sepuluh November
Surabaya, Indonesia
riyanarto@its.ac.id

Nur Setiawan Suroto
Department of Neurosurgery
Universitas Airlangga
Surabaya, Indonesia
nur.setiawan.suroto-2016@fk.unair.ac.id

Muhammad Ibadurrahman Arrasyid Supriyanto
Department of Informatics
Institut Teknologi Sepuluh Nopember
Surabaya, Indonesia
7025231002@student.its.ac.id

Gerry Sihaj
Department of Informatics
Institut Teknologi Sepuluh Nopember
Surabaya, Indonesia
6025222016@student.its.ac.id
Nur Setiawan Suroto

Rahadian Indarto Susilo
Department of Neurosurgery
Universitas Airlangga
Surabaya, Indonesia
rahadian-i-s@fk.unair.ac.id

2025 International Conference on Computer Sciences, Engineering, and Technology Innovation (ICoCSETI) | 979-8-3315-0861-6/25/$31.00 ©2025 IEEE | DOI: 10.1109/ICoCSETI63724.2025.11018970

***Abstract* — This study explores the effect of Anterior Commissure - Posterior Commissure (AC-PC) reorientation on 3D aneurysm segmentation accuracy in brain MRI (Magnetic Resonance Imaging) using the UNetR (UNet with Transformers) model. Accurate segmentation is critical in diagnosing life-threatening conditions like hemorrhagic stroke from aneurysm rupture. Given the importance of consistent imaging, AC-PC landmarks serve as valuable reference points for enhancing alignment. We conducted two preprocessing experiments: (1) reshaped to (256, 256, 256), and (2) reshaped to (256, 256, 256) with rotation based on the AC-PC line. Each experiment was evaluated by Dice score coefficient, yielding average scores of 0.22 (SD=0.19), and 0.24 (SD=0.21), respectively. While a paired t-test showed no statistically significant effect from AC-PC reorientation, the rotated data produced an approximate 9.4% improvement in segmentation accuracy. These findings suggest that incorporating AC-PC alignment may contribute to more reliable aneurysm segmentation in brain MRI, supporting the broader use of spatial reorientation to enhance diagnostic accuracy in AI-driven medical imaging**

Keywords* — *Brain Aneurysm, Segmentation, Deep Learning, Brain Landmarks, Medical Image Preprocessing

I. INTRODUCTION

MRI is commonly used by radiologists for detecting brain anomalies due to its superior spatial resolution, clear visualization [1], and non-invasive nature [2]. MRI is preferred for its high contrast and detailed imaging capabilities [2]. Advances in technology have enabled artificial intelligence (AI) to assist doctors in diagnosing diseases from medical images. One of the most widely used AI methods in medical image segmentation is Convolutional Neural Networks (CNN) such as UNet and its variations

Accuracy and precision of the diagnosis results are critical, as small differences in interpretation can result in different final prediction results. Shifting analysis from humans to machines will minimize the risk of errors caused by fatigue, reducing the potential for errors in the analysis of patient data. Machines can work tirelessly, avoiding performance degradation that affects doctors over time. One medical condition that can now be detected more accurately using MRI technology and AI is stroke.

Stroke is a serious condition caused by the blockage of blood vessels in the brain, leading to a reduced supply of oxygen and nutrients [1]. According to the WHO (World Health Organization), stroke is the second leading cause of death globally, accounting for 11% of all deaths and this number is still expected to increase over time [1]. If not treated appropriately, stroke can cause serious long-term effects, including disability, permanent brain damage, or even death [1]. One of the most dangerous types of stroke is hemorrhagic stroke, or more commonly known as a ruptured aneurysm, this medical condition occurs when a blocked blood vessel in the brain ruptures and results in internal bleeding in the brain [2].

Aneurysms are swollen blood vessels in the brain that, if not treated properly, can rupture and cause potentially fatal internal bleeding [3]. Most aneurysms do not rupture or cause negative symptoms, so they are often only detected accidentally during screening for other medical conditions [3]. Aneurysms occur in 1-2% of the population, but when focused on adults, the figure increases to 1-5%, with 50-80% of detected aneurysms not rupturing during a person's lifetime [4]. A study showed that in 82% of patients, the risk of aneurysm rupture was only 0.2%, while in another 18% of patients, the aneurysm enlarged, increasing the risk of rupture to 2.4% [4].

Given the critical need for precision in detecting and segmenting aneurysms, accurate image alignment plays a significant role in ensuring consistent results across MRI scans. The brain's anatomical landmarks, particularly the Anterior Commissure (AC) and Posterior Commissure (PC), serve as key reference points. These commissures are bundles of axons that enable communication between the brain's two hemispheres, with the AC and PC being key examples [5]. Identifying these two points is important because the line drawn between them can serve as a reference for orientation and localization in the brain [6] [7]. During the imaging process, several factors can contribute to tilting in the resulting scan, such as movement of subject's head during scanning and operator inexperience [8]. Therefore, these two points can ensure the accuracy of the position of the entire brain image to be analyzed.

This study will explore the impact of image reorientation based on the AC and PC landmark towards the performance of an aneurysm segmentation model. By utilizing this preprocessing technique, it can hopefully help well performing brain medical image segmentation models to perform even better. This paper is divided into key sections: Introduction (Section 1) provides background, problem statement, and objectives. Related Works (Section 2) outlines previous researches in a similar category. Section 3 covers Research Methods, detailing dataset, preprocessing, augmentation, and model used. Implementation and Results (Section 4) covers hyperparameters used for training as well as the final result of this research. Section 5 covers the conclusion of this research.

II. RELATED WORKS

Improving deep learning model performance has long been a focus, especially in fields with limited data like medical imaging. These improvements often come from data augmentation, preprocessing, or developing more robust models. With advancements in generative AI, synthetic data can now be created to enhance training datasets. In the medical field, where training data is limited, techniques like data preprocessing, augmentation, and synthetic data generation are essential for achieving performance levels similar to other domains. Below are notable works on these techniques that have improved medical image segmentation.

Previous research shows that various transformations and augmentations can improve segmentation. Converting images from Cartesian to polar format, for example, improves 2D segmentation for Polyp, Liver, Kidney, and EAT datasets [9]. GAN-generated synthetic images and histogram equalization have enhanced 3D segmentation for spleen, liver, and kidney datasets [10]. Another approach, simulating tissue deterioration through local image warping, also improves performance [11]. However, in microscopic segmentation, augmentations such as random scaling and noise addition may reduce the model's performance [12]. For breast cancer segmentation in ultrasound images, cutting and mirroring have shown to be beneficial [13]. Additionally, spatial normalization with attention mechanisms in the UNet++ architecture has significantly boosted segmentation on Synapse and CAMUS datasets [14].

While most studies focus on augmentations and transformations, limited research has explored anatomical reorientation techniques like AC-PC alignment. Common preprocessing methods often overlook brain-specific structural features that reorientation could exploit, potentially limiting segmentation accuracy. This study addresses this by examining how AC-PC reorientation affects 3D aneurysm segmentation, aiming to improve detection accuracy through anatomical alignment. By investigating this approach, this study seeks to highlight the importance of anatomical context in segmentation accuracy and its potential to optimize results in clinical applications

III. METHOD

The data for this research was sourced from the ADAM (Aneurysm Detection and segMentation) challenge, a comprehensive dataset used specifically for aneurysm detection and segmentation tasks. Preprocessing steps, including resizing, normalization, and AC-PC line-based rotation reorientation, were applied to prepare the dataset for optimal model performance. Data augmentation techniques, such as rotation, intensity shift, scaling, and random cropping, were also used to enhance model robustness. These preprocessing and augmentation methods aim to create a reliable dataset for evaluating the impact of AC-PC reorientation on 3D aneurysm segmentation accuracy

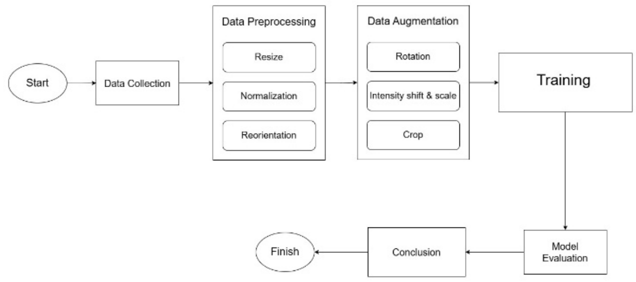

Fig 1. Research workflow

A. Data

The ADAM Challenge dataset was utilized for both training and validation. The dataset consists of medical images utilized solely for the purpose of aneurysm segmentation tasks. ADAM consists of 113 dataset, consisting of 20 healthy samples and 93 samples with manually segmented aneurysms. The dataset consists of 2 modality, ToF (Time of Flight) and structural MRI which can be either T1, T2, or FLAIR

The ADAM dataset's TOF (Time of Flight) modality is used for model training, with a sample shown in Fig 2. This non-invasive Magnetic Resonance Angiography (MRA) technique visualizes blood vessels without contrast agents [15]. TOF MRA achieves vessel contrast through fresh blood inflow into the imaging slice, enhancing visibility [15]. However, it requires a long acquisition time, especially for high spatial resolution [15]. This data modality is widely used to assess cerebral vasculature and diagnose vascular conditions such as occlusions, aneurysms, and arteriovenous malformations [15].

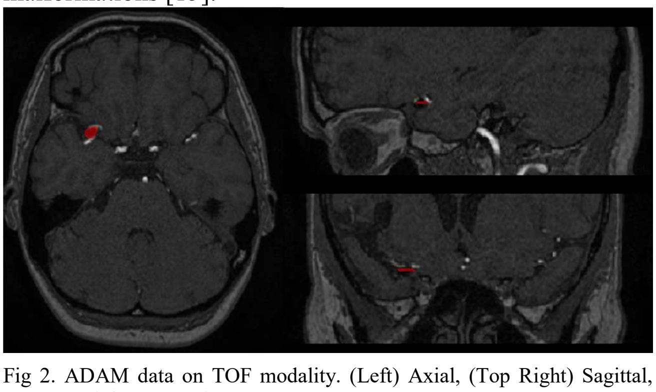

Fig 2. ADAM data on TOF modality. (Left) Axial, (Top Right) Sagittal, (Bottom Right) Coronal

B. Data Preprocessing

The data provided by the ADAM challenge was taken from many machines without proper standarizations, thus there are many variations in the data which first needs to be standarized. These standarizations consists of resizing and normalization. Aside from those two preprocessing method, we also propose a preprocessing technique in regards to the brain orientation based on 2 landmarks in the brain callled AC (Anterium Commisure) and (Posterior Commisure)

The dataset contains various dimension sizes, such as (512, 512, 140), (560, 560, 140), (512, 512, 100), and (1024, 1024, 160). To ensure consistency, the data is resized using the Resize function in the MONAI package, a package specializing in utilizing artificial intelligence for medical purposes. The resizing uses trilinear interpolation for ToF data and nearest interpolation for labels. The dataset was resized to (256, 256, 256), as this resolution is required by the landmark detection model used for reorientation.

After resizing, the data will be normalized to a range of [0,1], as the original intensity values vary across datasets (e.g., [0, 762], [0, 823], [0, 573], [0, 2764]). Normalization is crucial because the importance of an intensity value can differ depending on the dataset's intensity range. For example, an intensity of 150 in a range of [0, 200] is more significant than the same value in a range of [0, 750]. Normalization equalizes the intensity range across all datasets, ensuring each intensity value holds the same importance..

A previous research has produced a function to detect 2 landmarks in the brain namely AC and PC [16]. In an upright brain image, both landmark will exist in the same sagittal plane [17], thus this fact can be used as basis for rotating the image in the X and Z axis. In order to calculate the X and Z axis rotational angle, the dot product formula can be utilized resulting in (1) and (2)

$$rot(X) = \cos^{-1}\left(\frac{y_1 \times y_2 + z_1 \times z_2}{\sqrt{y_1^2 + z_1^2} \times \sqrt{y_2^2 \times z_2^2}}\right) \tag{1}$$

$$rot(Z) = \cos^{-1}\left(\frac{x_2 \times x_3 + y_2 \times y_3}{\sqrt{x_2^2 + y_2^2} \times \sqrt{x_3^2 \times y_3^2}}\right) \tag{2}$$

Where the original PC landmark is located at (x_1, y_1, z_1) and the resulting PC landmark after X axis rotation is located at (x_2, y_2, z_2) where $x_1 = x_2$, $rot(X)$ is the angle of rotation in the X axis, the resulting PC landmark after Z axis rotation is located at (x_3, y_3, z_3) where $z_2 = z_3$, and $rot(Z)$ is the angle of rotation in the Z axis

Finally, in order to perform the rotation on the dataset, the Rotate function from MONAI package was utilized. The function will take in the angles in radian for rotation and then rotate the image accordingly. The function's interpolation uses bilinear for the ToF data and nearest for the labels.

C. Data Augmentation

Due to the relatively small sample size for training, data augmentation needs to be done in order to produce a more robust model. Data augmentation is done through the transforms class in MONAI package. There are 4 augmentation functions utlilized for training, these augmentations consists of RandRotate, RandScaleIntensity, RandShiftIntensity, and RandCropByPosNegLabel.

RandRotate will randomly rotate both the image and label by a certain degree in each axis. For this experiment, it will have a 40% chance on each data to perform a rotation with degrees varying from -30 to 30 degrees on each axis. For interpolation, it uses the bilinear method for the image and nearest for the label.

RandScaleIntensity will randomly multiply the intensity of all the voxels in an image by a certain value. For this experiment, it will have a 30% chance on each data to multiply all its voxel intensity by a random value ranging from -0.1 to 0.1. On the other hand, RandShiftIntensity will randomly add a certain value to the intensity of all the voxels in an image. For this experiment, it will have a 30% chance on each data to increase the intensity of all its voxel by a random value ranging from -0.1 to 0.1

RandCropByPosNegLabel will randomly crop an image into smaller sizes where it has a chance to either choose either a foreground voxel (label 1) or a background voxel (label 0). This chance is entirely based on the positive and negative ratio used as parameters for the function. This experiment will randomly crop the image into size (128, 128, 128) with 4 samples and a 50% chance to select a foreground voxel compared to a background voxel. This augmentation was selected as it takes up a lot of memory to load the entire image at once so the data must first be cropped before loading.

D. UNETR (UNet Transformer)

This study employs UNetR, a transformer-based variant of the UNet model with an encoder-decoder structure that integrates transformers in the encoder for enhanced segmentation performance [18]. The encoder in UNetR starts with a patch embedding layer that divides the image into non-overlapping patches, which are then linearly embedded and passed through transformer layers applying multi-head self-attention and multilayer perceptrons to capture contextual information [19]. The decoder retains the traditional UNet upsampling and convolution approach to restore spatial dimensions, with skip connections transferring features from the encoder through transformer layers to improve spatial detail preservation [19] and improve segmentation accuracy by propagating essential early features [20]. After the decoder, two additional convolutional layers are applied, followed by a 1x1x1 convolution layer with softmax activation for voxel-wise predictions, ensuring accurate segmentation [19]. The full architecture of UNetR can be seen in Fig 3.

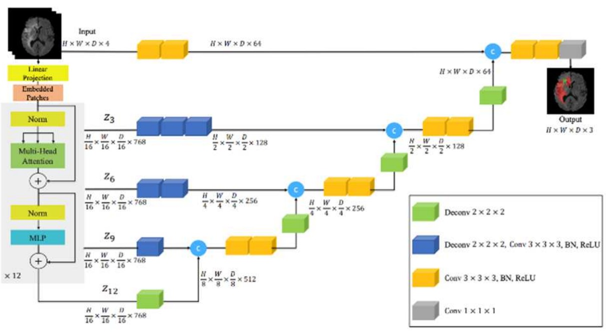

Fig 3. UNetR Architecture [19]

E. Loss Function

This research utilizes Dice Loss as its loss function, based on the Dice Similarity Coefficient (DSC), a widely used metric in segmentation tasks for measuring similarity between two data [21]. DSC values range from 0 to 1, where scores closer to 1 indicate high similarity and scores near 0 indicate dissimilarity. Equation (3) can be used to calculate the DSC of 2 data

$$DSC = \frac{2 \times |A \cap B|}{|A \cup B|} \tag{3}$$

Where A and B are the 2 data being compared.

Alternatively, it can be computed from a confusion matrix with (4)

$$DSC = \frac{2 \times TP}{2 \times TP + FP + FN} \tag{4}$$

Where TP (True Positive), FP (False Positive), and FN (False Negative) are the metrics derived from a confusion matrix as can be seen in Fig 4 [22].

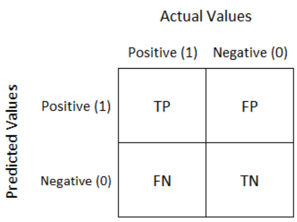

Fig 4. Confusion Matrix [23]

As Dice Loss is a minimization objective, it is calculated as (5), encouraging higher similarity scores between segmented output and ground truth

$$Loss = 1 - DSC \tag{5}$$

IV. Implementation and Result

A. Training

ADAM dataset consists of 113 data, a split for training and validation is performed in a 80-20 ratio, thus this model is trained on 90 data with the other 23 data reserved for validation. The data splitting process is done completely randomly, however each experiment will use the same data split.

For this research, the UNetR model was implemented using the MONAI package, which specializes in AI for medical applications. The model takes 3D grayscale input with 1 channel and produces binary classification output with 1 channel, using input data shaped (128, 128, 128). The base feature size for the U-Net structure is 16, with channels doubling at each downsampling step. To enhance feature representation, a hidden dimension of 768 is used in the transformer blocks, and the MLP layers have a dimensionality of 3072. Multi-head self-attention is applied with 12 heads to capture complex spatial dependencies. Perceptron-based projection is used, and instance normalization ensures consistent feature maps across channels. Sigmoid activation is applied at the output for binary classification, and the Adam optimizer is used with a learning rate of 0.0001 and weight decay of 0.00001. The model was trained for 1000 epochs with a batch size of 1.

B. Result

Fig. 5 shows the training loss progression across epochs for two models: one on 256x256x256 data (blue), and one on 256x256x256 data with additional rotation based on the AC-PC line (green). Initially, the loss values appear noisy due to optimization variability, but they were smoothed with a 100-epoch moving average to clarify the trends and improve clarity. This smoothing reveals each model's learning trajectory and convergence patterns, offering a clearer view of training stability. It also aids in identifying potential issues such as overfitting or underfitting, which are crucial for model refinement.

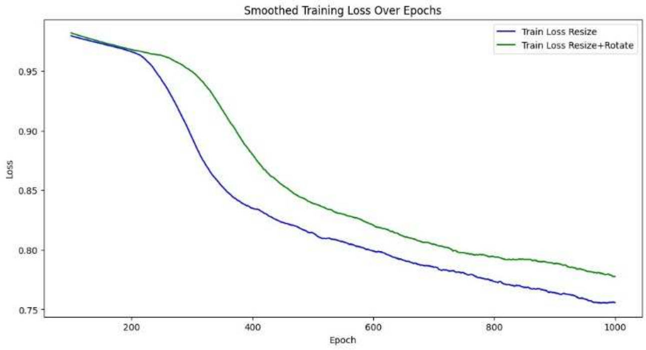

Fig 5. Training Loss Graph

Fig. 6 displays the Dice Score progression on the validation set across epochs for both models. The Dice scores were smoothed with a 100-epoch moving average to minimize fluctuations, providing a clearer view of the model's segmentation accuracy. At 1000 epochs, the graph shows that the dice scores averages out at around 0.20 for the data which was resized to 256x256x256 and then rotated, whilst for the data only resized to 256x256x256 it averages at around 0.175. This comparison highlights the impact of rotation on segmentation performance for the resized datasets

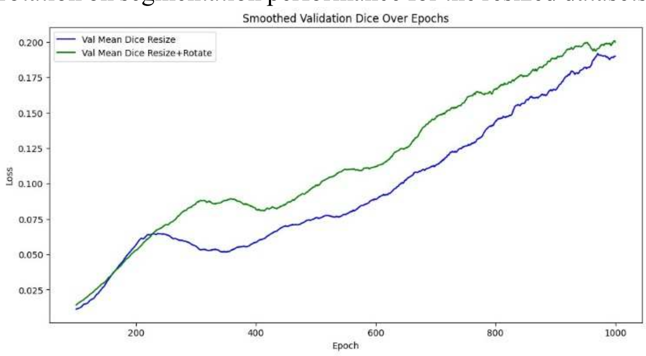

Fig 6. Validation Dice Graph

After training, the model with the highest validation Dice score from each version was selected for inference. Each model then performed inference on the validation dataset, with the Dice score from each run calculated and recorded for further analysis. The aggregated Dice scores are shown in Fig. 7, revealing an average score increase of 9.4% when reorientation is applied to the dataset

DSC	(256, 256, 256)	(256, 256, 256) + Rotate
Mean	0.22288	0.24381
Standard Deviation	0.19902	0.21409

Fig 7. Dice Validation Score

In order to assess whether rotational preprocessing affects the results, a paired T-test was conducted on the dice scores from both inference versions. The test revealed that rotation did not significantly impact the results, with a p-value of 0.423 for the comparison between the resized 256x256x256 version and the resized+rotated 256x256x256 version

V. Conclusion

This study did not find any significant impact in the performance of the model trained on the dataset after AC-PC reorientation. After a paired T-test between the dice score before and after reorientation, the p-value was found to be 0.423 indicating no significant impact of the reorientation treatment. However, if looked at an individual basis, reorientation does provide a better overall dice score as it gives an average score of 0.244 compared to not reorienting's average dice score of 0.225. Those numbers show that after reorientation is applied during the preprocessing phase, the dice score can increase by 9.4% on average

Acknowledgment

This research was funded by Institut Teknologi Sepuluh Nopember (ITS) under Penelitian Dana Departemen Program, Penelitian Keilmuan, Penelitian Flagship, Penelitian Kolaborasi Pusat and under the Project Scheme of the Publication Writing and Intellectual Property Rights (IPR) Incentive (Penulisan Publikasi dan Hak Kekayaan Intelektual/PPHKI) Program 2024.

References

[1] M. Ashrafuzzaman, S. Saha and K. Nur, "Prediction of Stroke Disease Using Deep CNN Based Approach," *Journal of Advances in Information Technology,* vol. 13, no. 6, pp. 604-613, December 2022.

[2] S. N. Ohashi, J. H. DeLong, M. G. Kozberg, D. J. Mazur-Hart, S. J. v. Veluw, N. J. Alkayed and L. H. Sansing, "Role of Inflammatory Processes in Hemorrhagic Stroke," *Stroke,* vol. 54, no. 2, pp. 605-619, February 2023.

[3] H. H. Karadeli and E. Kuram, "Single Component Polymers, Polymer Blends, and Polymer Composites for Interventional Endovascular Embolization of Intracranial Aneurysms," *Macromolecular Bioscience,* vol. 24, no. 5, May 2024.

[4] N. Ajiboye, N. Chalouhi, R. M. Starke, M. Zanaty and R. Bell, "Unruptured Cerebral Aneurysms: Evaluation and Management," *The Scientific World Journal,* vol. 2015, no. 4, 4 June 2015.

[5] K. B. Prakash, Q. Hu, A. Aziz and W. L. Nowinski, "Rapid and Automatic Localization of the Anterior and Posterior Commissure Point Landmarks in MR Volumetric Neuroimages," *Academic Radiology,* vol. 13, no. 1, pp. 36-54, January 2006.

[6] S. Minoshima, R. A. Koeppe, M. A. Mintun, K. L. Berger, S. F. Taylor, K. A. Frey and D. E. Kuhl, "Automated detection of the intercommissural line for stereotactic localization of functional brain images," *Journal of Nuclear Medicine,* vol. 34, no. 2, pp. 322-329, February 1993.

[7] Y. Xulei, T. W. Teng, T. Gabriel, Y. S. Yong and S. Yi, "Automatic detection of anatomical landmarks in brain MR scanning using multi-task deep neural networks," *Neurocomputing,* vol. 396, pp. 514-521, 5 July 2020.

[8] P. Prabhu, A. K. Karunakar, S. Sinha, N. Mariyappa, J. V. G. K. Bhargava and H. Anitha, "Content-Based Estimation of Brain MRI Tilt in Three Orthogonal Directions," *Journal of Digital Imaging,* vol. 34, p. 760–771, 24 February 2021.

[9] M. Benčević, I. Galić, M. Habijan and D. Babin, "Training on Polar Image Transformations Improves Biomedical Image Segmentation," *IEEE Access,* vol. 9, pp. 133365-133375, 2021.

[10] V. Sandfort, K. Yan, P. J. Pickhardt and R. M. Summers, "Data augmentation using generative adversarial networks (CycleGAN) to improve generalizability in CT segmentation tasks," *Scientific Reports,* vol. 9, 15 November 2019.

[11] H. Liu, H. Cao, E. Song, G. Ma, X. Xu, R. Jin, T. Liu, L. Liu, D. Liu and C.-C. Hung, "A new data augmentation method based on local image warping for medical image segmentation," *Medical physics,* vol. 48, no. 4, April 2021.

[12] J. Ma, C. Hu, P. Zhou, F. Jin, X. Wang and H. Huang, "Review of Image Augmentation Used in Deep Learning-Based Material Microscopic Image Segmentation," *Applied Sciences,* vol. 13, no. 11, 25 May 2023.

[13] C. Zhang, N. Bao, H. Sun, H. Li, J. Li, W. Qian and S. Zhou, "A Deep Learning Image Data Augmentation Method for Single Tumor Segmentation," *Frontiers in Oncology,* vol. 12, February 2022.

[14] A. A. Qurri and M. Almekkawy, "Improved UNet with Attention for Medical Image Segmentation," *Sensors,* vol. 23, no. 20, 2023.

[15] H. Tang, N. Hu, Y. Yuan, C. Xia, X. Liu, P. Zuo, A. F. Stalder, M. Schmidt, X. Zhou, B. Song and J. Sun, "Accelerated Time-of-Flight Magnetic Resonance Angiography with Sparse Undersampling and Iterative Reconstruction for the Evaluation of Intracranial Arteries," *Korean Journal of Radiology,* vol. 20, no. 2, pp. 265-274, 20 Feb 2019.

[16] K. N. Aisyah, C. Fatichah and R. Sarno, "Multilevel thresholding and Morphological Relationship Approach for Automatic," *International Journal of Intelligent Engineering and Systems,* vol. 13, no. 5, pp. 368-378, 17 July 2020.

[17] Y. Liu and B. M. Dawant, "Automatic Localization of the Anterior Commissure, Posterior Commissure, and Midsagittal Plane in MRI Scans using Regression Forests," *IEEE Journal of Biomedical and Health Informatics,* vol. 19, no. 4, pp. 1362 - 1374, July 2015.

[18] M. Gillot, B. Baquero, C. Le, R. Deleat-Besson, J. Bianchi, A. Ruellas, M. Gurgel, M. Yatabe, N. A. Turkestani, K. Najarian, R. Soroushmehr, S. Pieper, R. Kikinis, B. Paniagua, M. I. J. G. C. M. L. G. Heesoo Oh, Karine Evangelista, Cauby Maia Chaves Junior , Daniela Garib , Fábio Costa , Erika Benavides , Fabiana Soki , Jean-Christophe Fillion-Robin , Hina Joshi , Lucia Cevidanes and Juan Carlos Prieto, "Automatic multi-anatomical skull structure segmentation of cone-beam computed tomography scans using 3D UNETR," *PLoS One,* vol. 17, no. 10, 12 October 2022.

[19] A. Hatamizadeh, Y. Tang, V. Nath, D. Yang, A. Myronenko and B. Landman, "UNETR: Transformers for 3D Medical Image Segmentation," in *2022 IEEE/CVF Winter Conference on Applications of Computer Vision (WACV)*, 2022.

[20] N. Zioulis, G. Albanis, P. Drakoulis, F. Alvarez, D. Zarpalas and P. Daras, "Hybrid Skip: A Biologically Inspired Skip Connection for the UNet Architecture," *IEEE Access,* vol. 10, pp. 53928-53939, 2022.

[21] A. S. Nugroho, A. Fajar, R. Sarno, C. Fatichah, A. Fahmi and S. A. Utomo, "Unsupervised Method for 3D Brain Magnetic Resonance Image Segmentation," in *2021 IEEE Asia Pacific Conference on Wireless and Mobile (APWiMob)*, 2021.

[22] Y.-H. Nai, B. W. Teo, N. L. T. S. O. M. C. Stephenson, Y. L. Thian, E. Chiong and A. Reilhac, "Comparison of metrics for the evaluation of medical segmentations using prostate MRI dataset," *Computers in Biology and Medicine,* vol. 134, 2021.

[23] Shylaja and H. N, "A REVIEW OF COMPUTATIONAL BIOLOGY APPROACHES IN AGRICULTURE," in *INFORMATION TECHNOLOGY & BIOINFORMATICS: INTERNATIONAL CONFERENCE ON ADVANCE IT, ENGINEERING AND MANAGEMENT - SACAIM-2022*, 2023.